Polymer 52 (2011) 1619–1627

Contents lists available at ScienceDirect

Polymer

journal homepage: www.elsevier.com/locate/polymer

Carbon dioxide plasticization and conditioning effects in thick vs. thin glassy polymer films

Norman R. Horn, D.R. Paul*

Department of Chemical Engineering and Texas Materials Institute, The University of Texas at Austin, Austin, TX 78712, United States

ARTICLE INFO

Article history:
Received 23 November 2010
Received in revised form
1 February 2011
Accepted 5 February 2011
Available online 12 February 2011

Keywords:
Plasticization
Thin films
Gas permeability

ABSTRACT

Recent studies have shown that thin glassy polymer films undergo physical aging more rapidly than thick films. This suggests that thickness may also play a role in the plasticization and conditioning responses of thin glassy films in the presence of highly-sorbing penetrants such as CO_2. In this paper, a carefully designed systematic study explores the effect of thickness on the CO_2 plasticization and conditioning phenomena in Matrimid®, a polyimide commonly used in commercial gas separation membranes. Thin films are found to be more sensitive than thick films to CO_2 exposure, undergoing more extensive and rapid plasticization at any pressure. The response of glassy polymers films to CO_2 is not only dependent on thickness, but also on aging time, CO_2 pressure, exposure time, and prior history. Finally, thin films experiencing constant CO_2 exposure for longer periods of time exhibit an initial large increase in CO_2 permeability, which eventually reaches a maximum, followed by a significant decrease in permeability for the duration of the experiment. Thick films, in contrast, do not seem to exhibit this trend for the range of conditions explored.

1. Introduction

At temperatures greater than the glass transition temperature (T_g), amorphous polymers are nearly always in a state of physical equilibrium, and their gas permeation properties at low sorption levels are characterized by constant permeability, diffusivity, and solubility coefficients. High sorption levels of more soluble gases, such as CO_2, can "plasticize" these polymers, resulting in an increase in permeability and diffusivity with concentration [1]. These effects are reversible upon removal of penetrant, with no observable time and thickness effects. The gas concentration alone determines the transport properties.

In contrast, a polymer below T_g is in a non-equilibrium state, but for bulk polymers, i.e., thick films, the rate of progress toward equilibrium, termed physical aging, is very slow. At relatively low penetrant concentrations, permeation usually follows the dual-sorption – dual-mobility model [2] and the effects of penetrant sorption are mostly reversible over reasonable time periods. However, "plasticization" can occur at high penetrated concentrations owing to increased free volume that facilitates molecular motions and, thereby, increases the permeability of all gas species [3–7]. Once the plasticizer is removed, the polymer may not immediately return to its previous state, an effect sometimes called "conditioning" [8]. Conditioning is not immediately reversible, and all changes depend on the thermodynamic history and experimental conditions.

Most gas separation membranes are made of glassy polymers, and understandably the "plasticization" effect is very important as membrane technology is extended to cases where there are high partial pressures of penetrants that are highly soluble in the polymer, such as natural gas streams with high CO_2 contents. This is a very complex problem for several reasons. Practical membranes must be very thin, ~100 nm, in order to obtain high flux or productivity, but such thin structures are now well known to behave differently than thicker counterparts. For instance, gas transport through glassy polymers is significantly affected by physical aging. Physical aging has been extensively studied in bulk polymers [9], but films below ~1 micron in thickness exhibit greatly accelerated physical aging relative to the bulk state [10–17]. The reason for the thickness effect in thin films is not well-understood, but there is every reason to expect that thickness also plays a role in plasticization and conditioning behavior. Furthermore, plasticization and physical aging are competitive processes; as plasticization changes the state of the polymer, physical aging is perturbed, and vice versa.

Much effort has been expended studying CO_2 transport in thick glassy films, generally under the implicit assumption that the

* Corresponding author. Tel.: +1 512 471 5392; fax: +1 512 471 0542.
E-mail address: drp@che.utexas.edu (D.R. Paul).

0032-3861/$ – see front matter © 2011 Elsevier Ltd. All rights reserved.
doi:10.1016/j.polymer.2011.02.007

properties of thick films mimic those of thin films [18–22]. There have been a few investigations concerned with CO_2 plasticization in thin films, but systematic studies of this phenomenon are extremely limited. Berens [23–26] and Hopfenberg [27,28] studied gas sorption kinetics in polymer powders and suggested that particle size played some role in transport properties; however, they did not extensively study the size effect with plasticizing molecules. Wessling et al. and Zhou et al. observed accelerated plasticization in composite membranes and polyimide membranes, respectively, with thicknesses varying from 0.5 to 4 μm [29,30]. Zhou suggests that the so-called "plasticization pressure" is thickness dependent, in contrast with Pfromm [31]. Scholes et al. reported significant plasticization for thin films below the plasticization pressure and used an expanded dual-sorption model to fit their data [32]. Chung et al. also observed that the plasticization pressure was inadequate to determine the incipient point of plasticization, but their work focused on thicker films (~50 μm) [33]. Kim et al. described the effects of CO_2 exposure on thin 6FDA-based polyimide membrane systems [34–37]. Kratochvil et al. showed an unexpected decline in CO_2 permeability and sorption above the supercritical point of CO_2 for uncrosslinked 6F-based polyimide thick membranes, but did not see a decline for crosslinked membranes under similar conditions [38,39]. Lee et al. investigated how highly-sorbing organic vapors contaminants, such as toluene or n-heptane, affect the CO_2/CH_4 separation performance of Matrimid® hollow-fiber membranes [40,41]. Pandiyan, Neyertz, and coworkers performed CO_2 solubility, diffusion, and plasticization simulations consistent with prior experimental results, but the timescale of the simulation was only a few nanoseconds [42,43]. Most recently, Rowe et al. demonstrated that prior CO_2 exposure history plays an unusual role in physical aging behavior in thin polysulfone films [44]. Clearly, there is growing evidence that CO_2 effects on permeation behavior are thickness dependent.

The goal of this work is to explore how film thickness influences CO_2 plasticization and conditioning effects for glassy polymers used as gas separation membranes with carefully defined and controlled experiments. Having meaningful assessment techniques is essential for development of more robust membranes that provide high separation performance and are not unduly perturbed by the feed stream composition or operating conditions.

2. Experimental

Matrimid® 5218, a thermoplastic polyimide made from the monomers 3,3′,4,4′-benzophenone tetracarboxylicdianhydride (BTDA) and diaminophenylindane (DAPI), was used as received from Huntsman Advanced Materials for this study (Table 1). It has favorable high temperature properties for use in composites and adhesives and is soluble in many common solvents. Matrimid® was chosen because it is a commonly used material for commercial gas separation membranes, has a high T_g (310 °C) and, thus, is deep within the glassy state during normal use at ambient conditions, and is known to be plasticized by CO_2 to a significant extent. Thick Matrimid® films were prepared by casting solutions in dichloromethane on silicon wafers with a steel ring barrier within a sealed glove bag; thickness was controlled by varying the polymer concentration. A Dektak 6 M stylus profilometer was used to measure thickness for all thick films. Thin Matrimid® films were prepared by spin casting solutions in cyclohexanone onto silicon wafers at 1200 rpm for 90 s; thickness was controlled by varying the concentration of polymer from 3–6 wt.%. A variable angle spectroscopic ellipsometer (J.A. Woollam Co., model 2000D) was used to measure the thickness of all thin films.

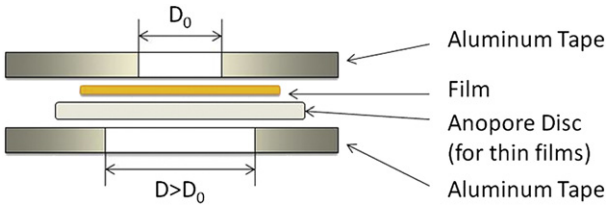

Fig. 1. Film masking schematic.

Gas transport studies for thin films are often hampered by the presence of microscopic pinhole defects, which allow undesirable convective flow to dominate gas flux and make a film non-selective. A defect fraction of 10^{-6} on an area basis is sufficient to render a film useless for gas separation [45]. However, coating a second layer of a highly-permeable polymer such as poly(dimethylsiloxane) (PDMS) directly on top of the selective glassy layer can mitigate defects by blocking convective flow [45]. At ambient conditions, PDMS is a rubbery polymer whose gas transport properties do not change with time due to physical aging. Rowe et al. have confirmed that PDMS has no significant effect on the glassy layer [46]. After spin-coating each thin Matrimid® film, a coating was applied by spin casting a PDMS/cyclohexane solution onto the glassy film at 1000 rpm for 60 s. The wafer was then placed on a hot plate and annealed at 110 °C for 15 min to crosslink the PDMS film and remove residual solvent. The PDMS solution consisted of Wacker Silicones Corporation Dehesive 940A and cyclohexane in a 2:3 ratio by volume, proprietary catalyst (OL), and crosslinking agent (V24). The thickness of the PDMS layer was ~4 μm as measured by a Dektak 6M stylus profilometer.

Any polymer film is imbued with a unique thermal history originating from the formation process, so all films were heated to 15 °C above the glass transition temperature of Matrimid® and annealed for 10 min, followed by a rapid temperature quench. This treatment erases prior thermal history and relaxes any orientation induced by the film formation process. Thus, all films are given a common history, allowing legitimate comparison for physical aging. Films were masked between two pieces of aluminum tape, supported by an Anopore™ disc for thin films (Fig. 1). All samples were aged in air at ambient pressure and 35 °C. Samples experienced no CO_2 exposure during the initial aging period. Pure gas

Table 1
Matrimid® properties.

Polymer	ρ (g/cm^3)	T_g (°C)	Refractive index
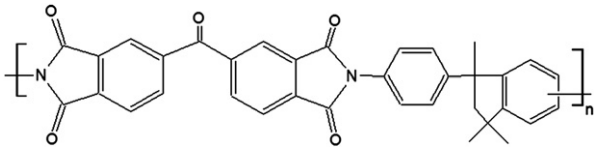 Matrimid® 5218	1.20	310	1.648

permeabilities were measured at 35 °C using a standard constant volume, variable pressure apparatus [47]. CO_2 gas was provided by Matheson Tri-Gas and was at least 99.99% pure. The upstream side of the permeation cell had a small, observable leak owing to the metal part connections, ensuring that accumulation of feed gas impurities could not occur.

A typical experiment for demonstrating CO_2 plasticization effects in a polymer film involves measuring CO_2 permeability as a function of upstream gas pressure. The literature abounds with polymer gas transport data for gases such as O_2, N_2, and CH_4 that follow the dual-sorption, dual-mobility model, which predicts a slight decrease in permeability with increasing pressure. However, plasticizing penetrants exhibit significant deviations from this behavior. At relatively low CO_2 pressures, the gas permeability of a glassy film decreases with increasing pressure, following the predicted behavior of the dual-mode model. As more CO_2 is sorbed, the polymer is plasticized, which leads to an upward inflection in the gas permeability curve as CO_2 pressure increases, and the minimum in this curve is often called the plasticization pressure. However, this term is somewhat misleading since plasticization occurs well below this pressure [32]. As will be demonstrated in this paper, CO_2-induced plasticization effects for thin films are pressure, time, and thickness dependent.

When conducting experiments on thin glassy films with CO_2, the results are greatly affected by the method chosen. Many variables must be taken into account: the pressure or concentration of CO_2 a film experiences, the exposure time a film spends at a particular CO_2 pressure, the aging time of the film both before and during CO_2 exposure, the film thickness, and any prior thermal or plasticization history. In the following results, all procedures will be explained in each subsection individually for clarity.

3. CO_2 permeation behavior for short exposure times

3.1. CO_2 plasticization pressure curves

As mentioned previously, plasticization is frequently depicted in the literature with plots showing the CO_2 permeability of a glassy polymer passing through a minimum, the so-called "plasticization pressure," as pressure increases. Fig. 2 displays such curves for a thick (~20 μm) and thin (~180 nm) Matrimid® film. The films were first aged for 100 h at 35 °C. In each experiment, the films were first exposed to 2 atm of CO_2 at the upstream side of the membrane. Pressure was incremented by 2 atm until reaching 20 atm, and then incremented by 4 atm until reaching 40 atm. Since the time lag for Matrimid® films with thickness of 15–35 μm ranges from 60 to 90 s, the steady state permeability at each pressure was measured after ~9 min of CO_2 exposure by monitoring the downstream pressure for ~60 s. The pressure was then immediately increased to the next set point. A film with thickness less than 1 μm, however, reaches steady state in a very short time, and, thus, the thin film was held at each pressure for only 3 min.

The thick film's plasticization pressure curve (Fig. 2) had the expected shape with a minimum at ~14 atm CO_2, which is consistent with the literature. The CO_2 permeability decreased by 22% from 2 atm to 14 atm, but the initial value was recovered by 36 atm. In contrast, the thin film's apparent plasticization pressure is ~6 atm, and CO_2 permeability decreased by only 6% from 2 atm to 6 atm. The permeability returned to its initial value by 14 atm and continued to increase markedly as pressure increased. At 40 atm, the permeability is nearly twice the initial value at 2 atm. The difference in shape of the curves suggests that the thin film experiences substantially more plasticization in short amounts of time, even at lower pressures.

3.2. Effect of thickness on CO_2 permeability hysteresis

A plasticization pressure curve provides some insight into a polymer's response to CO_2 as pressure is varied but is rather limited in describing the effect of CO_2 exposure for longer times. A modified plasticization pressure curve method was developed to capture these details, following a similar method from Puleo et al. [48]. The method involves four steps: 1. Pressurization from 2 atm to 32 atm CO_2, spending 10 min at each intermediate pressure; 2. Hold at 32 atm CO_2 for 4 h; 3. Depressurization from 32 atm to 4 atm CO_2, spending 10 min at each intermediate pressure; 4. Hold at 4 atm CO_2 for 12 h. This procedure was applied identically to a thick (~15 μm) and thin (~160 nm) Matrimid® film, each aged for 100 h at 35 °C. Permeability was measured multiple times for the thin film during the pressurization stage (at 2, 5, and 9 min) and depressurization stage (at 5 and 9 min). However, only one measurement was made at each pressure for the thick film, since the thick film's time lag is orders of magnitude greater than that of the thin film. More frequent measurements for thin films allow effects of CO_2 at short exposure times to become more evident.

Fig. 3 shows CO_2 permeability versus both pressure and time for the procedure described above. For the thick film, the pressurization step resembles the plasticization pressure curve in Fig. 2, but the plasticization pressure appears to have shifted to a higher pressure (~16–20 atm) and the film does not return to its initial permeability as quickly. This behavior is attributed to the greater incremental increases in pressure involved in the different procedure. Permeability increased in the 4 h hold step at 32 atm by 6.2%. The permeability continued to increase during the depressurization step, a phenomenon also observed in thick polystyrene [48], cellulose acetate [49], and polycarbonate [50] films. The polymer begins to relax toward its original state as penetrant is removed, but does not have sufficient time for significant relaxation and the dilated structure allows for greater gas flux. During the 12 h hold step at 4 atm the permeability decreases and approaches the curve generated during the pressurization cycle.

The thin film reasonably follows the shape of the plasticization pressure curve from Fig. 2, but the different procedure results in

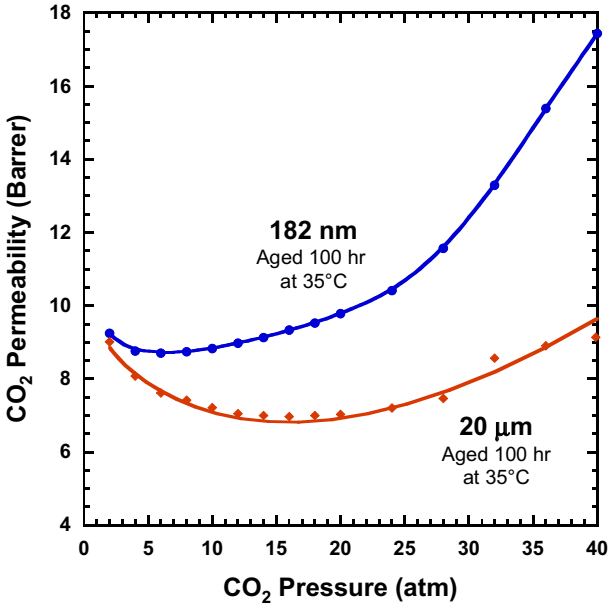

Fig. 2. CO_2 plasticization pressure curves for thin and thick films with identical prior thermal history. The thin and thick films spent 3 and 10 min, respectively, at each intermediate pressure.

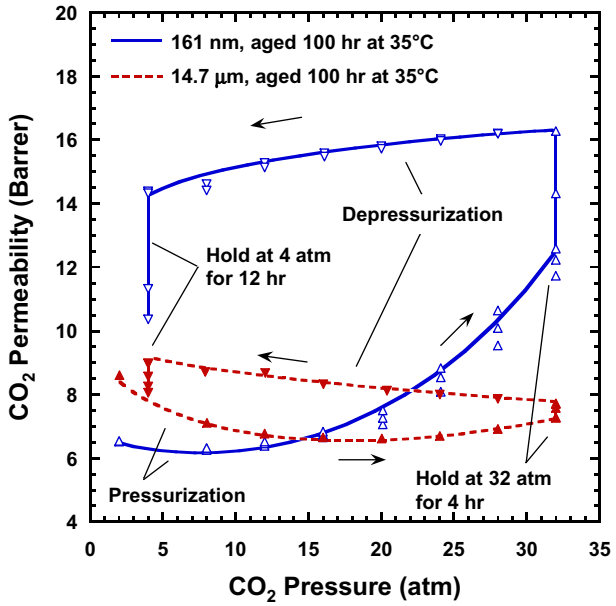

Fig. 3. CO_2 permeability hysteresis for thin and thick films with identical prior thermal history. Each film proceeds through four steps: 1. Pressurization from 2 atm to 32 atm, spending 10 min at each intermediate pressure; 2. Hold at 32 atm for 4 h; 3. Depressurization from 32 atm to 4 atm, spending 10 min at each intermediate pressure; 4. Hold at 4 atm for 12 h.

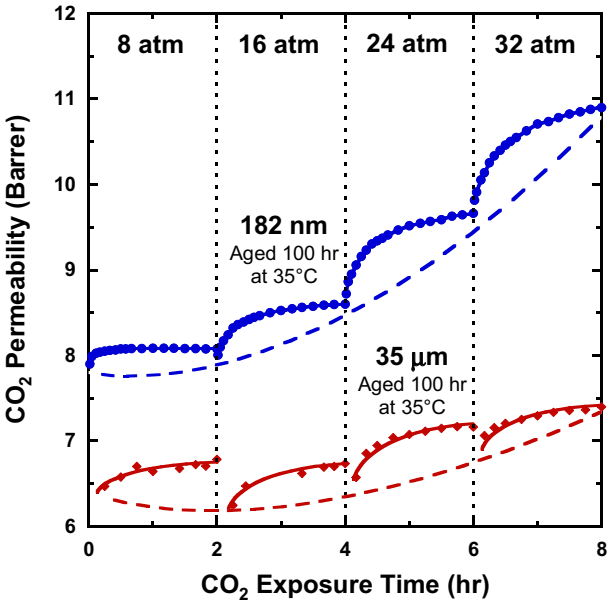

Fig. 4. Short time experiments for thin and thick films with identical prior thermal history.

slightly different permeability values at each pressure. At 20 atm in the pressurization step, measureable increases in permeability were observed within 10 min of exposure time. At 32 atm, permeability increased nearly 10% within 10 min of exposure time, and over the 4 h hold period at 32 atm increased 40%. Unlike the thick film, the permeability decreased during the depressurization step. This decrease is attributed to thin films having shorter relaxation times than thick films. Permeability continued to decrease significantly throughout the 12 h hold step at 4 atm CO_2, but did not return to the regressed curve for the pressurization step.

3.3. Short time CO_2 permeation experiments

The experiments in the previous sections show that thick and thin films respond differently to CO_2 under conditions of varying pressure and time. In this section, CO_2 permeability is tracked for a fixed time with fewer upstream pressure changes. Thick (~35 μm) and thin (~180 nm) Matrimid® films, each aged for 100 h at 35 °C, were exposed to a sequence of four CO_2 pressures for 2 h at each pressure: 8 atm, 16 atm, 24 atm, and 32 atm. This particular sequence was chosen to include pressures below and above the CO_2 plasticization pressure of Matrimid®, generally accepted to be 12–14 atm.

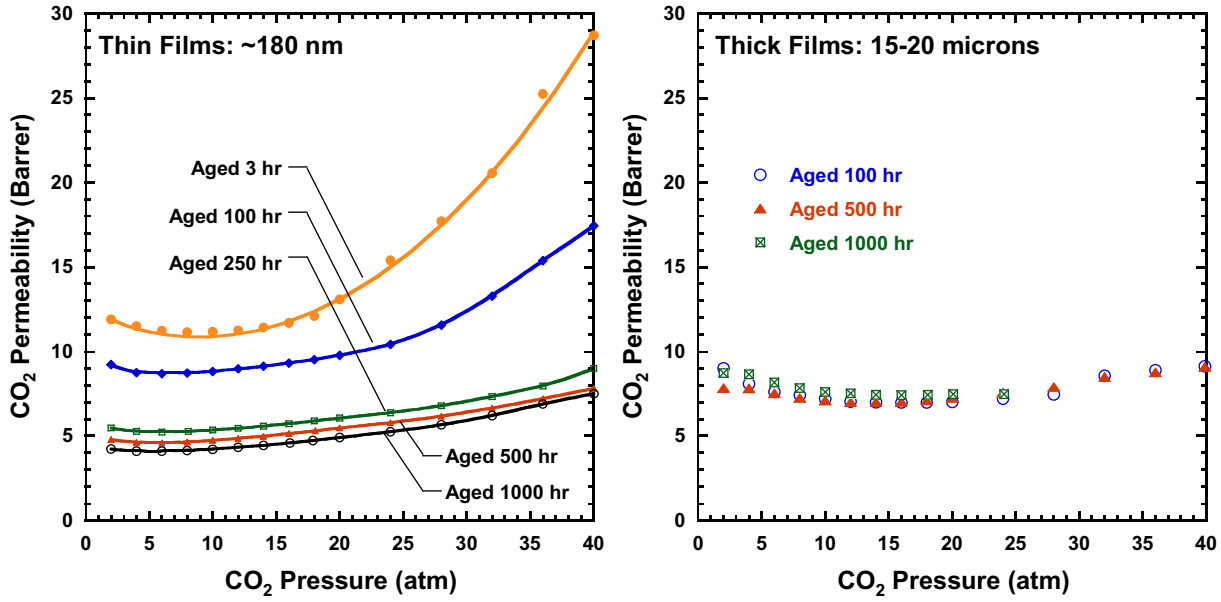

Fig. 5. Effect of aging time on plasticization pressure and CO_2 permeability for thin and thick films. Each data set represents a unique film aged in the absence of CO_2 until the specified aging time. The thin and thick films spent 3 and 10 min, respectively, at each intermediate pressure.

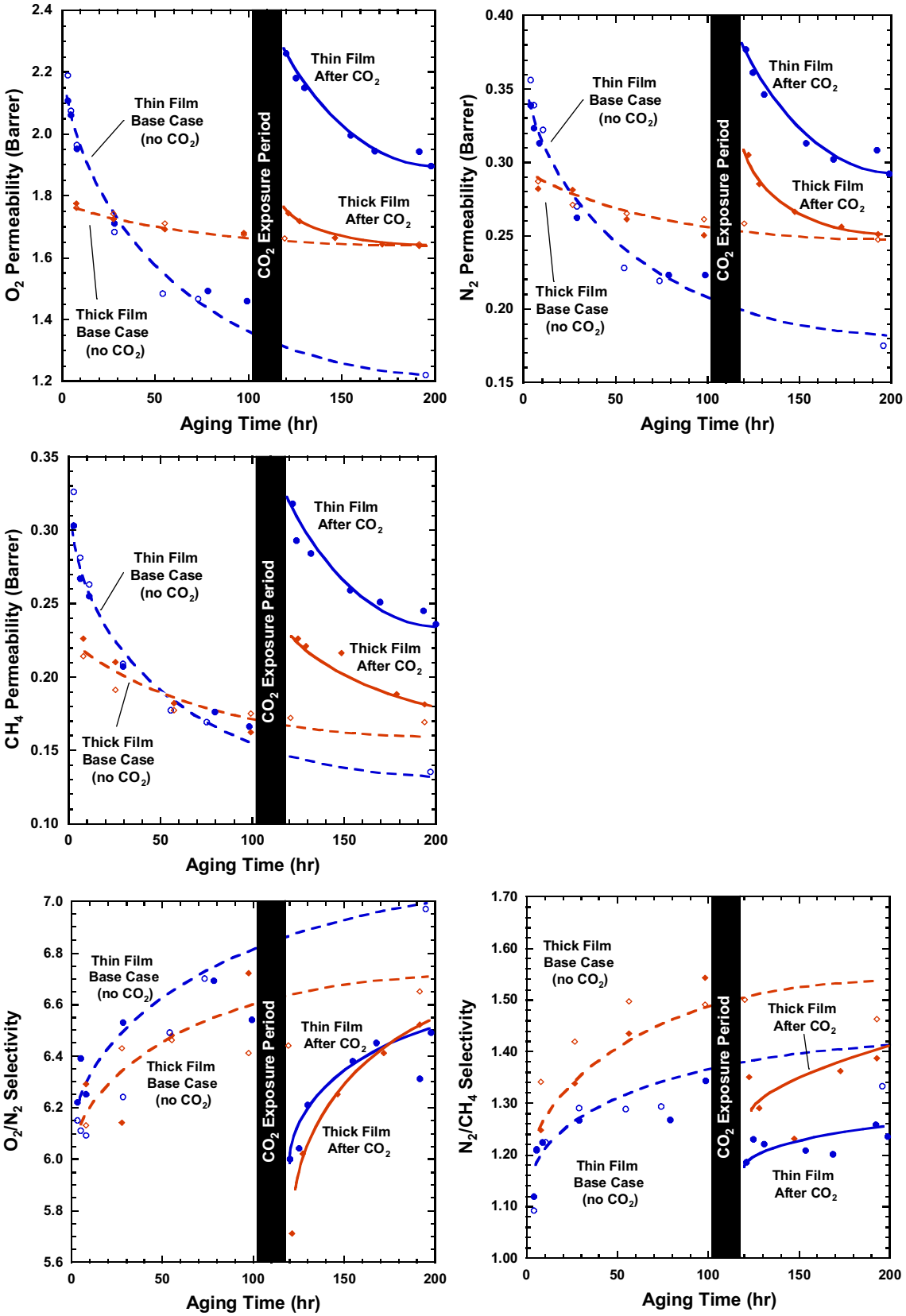

Fig. 6. CO_2 conditioning effects. (◇) Thin film base case, (◆) thin film with CO_2 exposure, (○) thick film base case, (●) thick film with CO_2 exposure. The CO_2 exposure period followed the procedure outlined in Section 3.2.

The responses of the thick and thin films tested with this procedure (Fig. 4) are quite different. Taking the first data point from each pressure for the thick film, one could construct a rudimentary plasticization pressure curve sufficiently consistent with prior observations. The thin film, however, exhibits a significant departure from behavior observed with previous methods. Much greater changes take place over short time periods, and the effect becomes more pronounced as pressure increases. For example, the CO_2 permeability for the thin film increased 38% from start to finish, while for the thick film the increase was 15%.

3.4. Effect of aging time on plasticization pressure and CO_2 permeability

Gas sorption and permeability in glassy polymers is directly related to the free volume, and free volume decreases as the polymer ages. Thus, physical aging should have an effect on how a polymer plasticizes in the presence of CO_2. A series of thick (~15–20 μm) and thin (~180 nm) films were prepared and aged at 35 °C. At set aging times a film was exposed to CO_2 according to the plasticization pressure curve procedure outlined in Section 3.1. More thin films were tested so that the effect of aging time could be more clearly seen.

Fig. 5 shows results of thick and thin films using the plasticization pressure curve procedure at different aging times. The three thick films, aged 100, 500, and 1000 h before testing, show little discernible difference between their plasticization pressure curves. This is attributed to the very slow physical aging of bulk glassy polymers; thus, aging does not seem to play a significant role in the plasticization response of bulk polymers. The thin films were aged 3, 100, 250, 500, and 1000 h before testing. As aging time increased, the plasticization pressure curve shifts to lower permeability and appears to flatten out. The effect of aging is more pronounced at short aging times. For instance, the downward shift of permeability from 3 h to 250 h aging is much greater than the shift from 250 h to 500 h, or from 500 h to 1000 h aging. This is a result of the more rapid aging rate and higher free volume state of thin films at short aging times. The plasticization pressure appears to decrease slightly with increased aging time. Furthermore, films aged for shorter amounts of time had greater relative changes in permeability as pressure was varied.

3.5. CO_2 conditioning effects

In addition to being plasticized by CO_2, glassy polymers can display rather long term changes associated with the CO_2 exposure, often called conditioning effects, once the CO_2 is removed. To document such behavior, the permeabilities of O_2, N_2, and CH_4 were measured for two thick (~20 μm) and two thin (~160 nm) films before and after CO_2 exposure, while the films were aging at 35 °C. After aging for 100 h, thick and thin films were exposed to CO_2 using the modified plasticization pressure curve method: each film experienced a pressurization step, a hold step at 32 atm CO_2, a depressurization step, and a hold step at 4 atm CO_2. Further details can be found in Section 3.2. The remaining films did not experience any CO_2 exposure and serves as the "base case." Upon completion of the CO_2 exposure period, the permeabilities of O_2, N_2, and CH_4 were tracked until the films had aged 200 h at 35 °C.

Fig. 6 includes permeability data for O_2, N_2, and CH_4 and selectivities calculated for O_2/N_2 and N_2/CH_4. The pure gas permeabilities of the thin films were all initially greater than those of the thick films, but even after aging 100 h the thin films showed significant decreases in permeability and the relative positions of the thick and thin films had reversed. Following CO_2 exposure, thick and thin film gas permeabilities increased considerably, but the thin film increased to a greater extent for each gas. Despite having shorter relaxation times the thin film did not return to the base case permeability within the time period of this experiment. The thick film, however, appeared close to returning to the base case after aging 200 h. The general behavior of the pure gas selectivities was consistent with predictions insofar as conditioning caused each selectivity to decrease, but it is difficult to discern any difference due to thickness within the limits of these observations.

4. CO_2 permeation behavior for long exposure times

The experiments described above employ relatively short CO_2 exposure times (<20 h). Most previous research in the literature

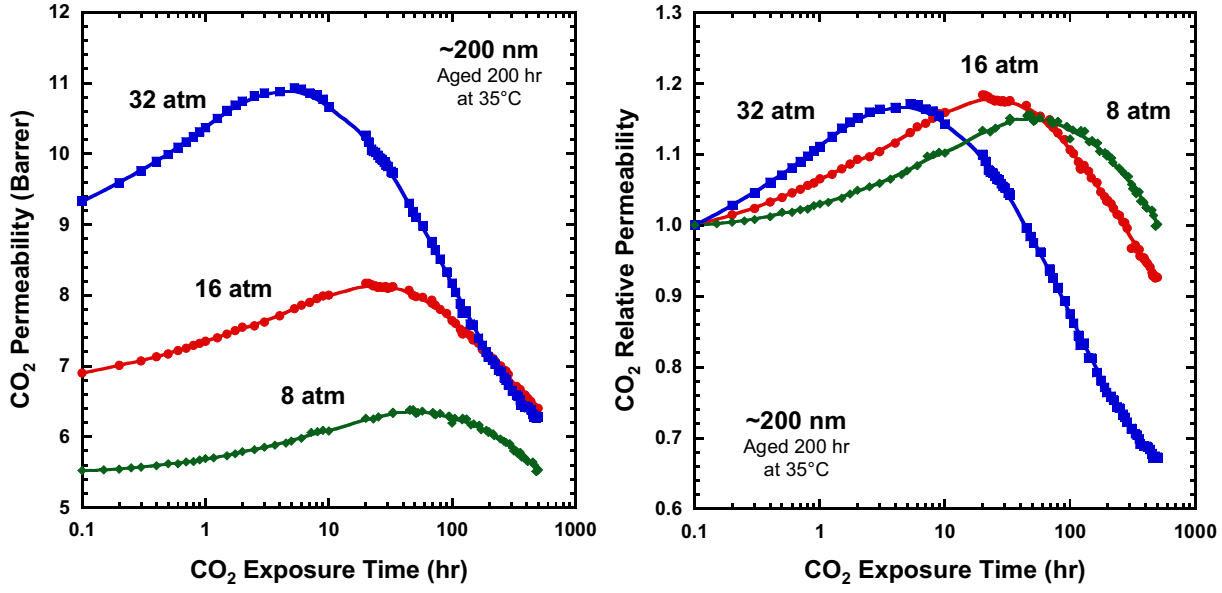

Fig. 7. Effect of long-time CO_2 exposure at constant pressure for thin films with identical thickness and prior thermal history.

tends to focus on thick films, shorter CO_2 exposure periods, and lower CO_2 pressures. However, such experiments could mask the effect that exposure to CO_2 might have for longer periods of time or at higher pressures. Further experiments were performed to explore these possibilities. Three thin films, all 200–220 nm thick, were aged for 200 h at 35 °C. The films were then exposed to CO_2 at constant pressure for 500 h, and CO_2 permeability was tracked throughout the exposure period. Similar to the experiments described in Section 3.3, the particular CO_2 pressures (8 atm, 16 atm, 32 atm) were chosen to include pressures below and above the CO_2 plasticization pressure of Matrimid®.

The literature suggests that such experiments will exhibit a significant increase in CO_2 permeability, asymptotically approaching a maximum. In contrast, these thin films behaved quite differently. As expected, the CO_2 permeability of each film, depicted in Fig. 7,increased significantly with time. However, after each film reached a permeability maximum, the trend reversed and the permeability decreased. At higher pressures, the permeability maximum occurred at shorter times and decreased to a greater extent by 500 h of CO_2 exposure. The permeability drop indicates that aging is the dominant process even though CO_2 is still present in the film. To our knowledge, such behavior has not previously been described in the literature for gas transport processes, since most experiments of this kind are performed at moderate pressures, with thicker films, and for less than 100 h of CO_2 exposure, all conditions where this phenomenon is not as prominent. This behavior even occurs below the plasticization pressure of Matrimid®, further confirming that significant plasticization does indeed take place in thin glassy films at any CO_2 pressure. Another interesting result is that each film has approximately the same maximum relative permeability, with lower CO_2 pressures requiring more time to reach the maximum. This similarity could be due to each film having aged the same amount of time before being tested. Following CO_2 exposure, O_2, N_2, and CH_4permeability were measured for each film. All permeability coefficients were below the respective values measured before CO_2 exposure, which is consistent with the hypothesis that physical aging out-competed plasticization at long CO_2 exposure times in these thin films.

The effect of aging time and thickness on CO_2 response at long exposure times was investigated using the same procedure. Fig. 8 shows permeation data for three films tested at 32 atm CO_2 for up to 1000 h. Included here is data for a 220 nm film, aged 200 h at 35 °C, from Fig. 7. A second film, 202 nm thick, was aged 800 h at 35 °C before CO_2 exposure, while a third film, 20 μm thick, was aged 200 h at 35 °C before CO_2 exposure.

Physical aging is a densification process resulting in a loss of free volume over time. Therefore, relative to a ~200 nm film aged 200 h at 35 °C, a film of comparable thickness aged longer and exposed to similar CO_2 conditions would show a decrease in the initial permeability of the film, the same maximum permeability as the previous film, and increased time until reaching a maximum absolute permeability. The expected behavior did occur, and in fact the maximum permeability of each film differed by 2%. The relative change from time zero to maximum permeability was 42%.

Paralleling the evidence in Section 3, these data suggest that thin films respond relatively more quickly and intensely to plasticizing gases, such as CO_2, than thick films. The data shown in Fig. 8 for thick and thin films, both aged 200 h at 35 °C, are consistent with these observations. After 5 h of CO_2 exposure at 32 atm, the CO_2 permeability of the thin film increased by 17%, passed through a maximum, and then sharply declined with further exposure time at constant pressure. In contrast, the permeability of the thick film increased by only 8% over 1000 h of CO_2 exposure at 32 atm. Though it is possible that the thick film could go through a maximum in permeability at a longer time or at significantly higher pressures (such as the supercritical CO_2 conditions tested by Kratochvil et al. [38,39]), no maximum was distinctly observed within the bounds of this experiment.

The behavior in Fig. 7 resembles the volumetric "memory effect" observed by Kovacs et al. [51] for temperature jumps about the glass transition of poly(vinyl acetate). Fig. 9 attempts to generalize the Kovacs experiment by schematically showing the volume relaxation of a glassy polymer at a fixed temperature, T_f, below the glass transition temperature, T_g, versus time at that temperature for various thermal histories. Curve 1 shows the case where the polymer is simply down-quenched from T_1, above T_g, to T_f. In all the other curves, the polymer was down-quenched from T_1 to T_i, held there for a certain time, and then up-quenched from T_i to T_f. These curves show the response of the volume versus time after arriving at T_f. Curve 1 shows a simple monotonic volume relaxation as

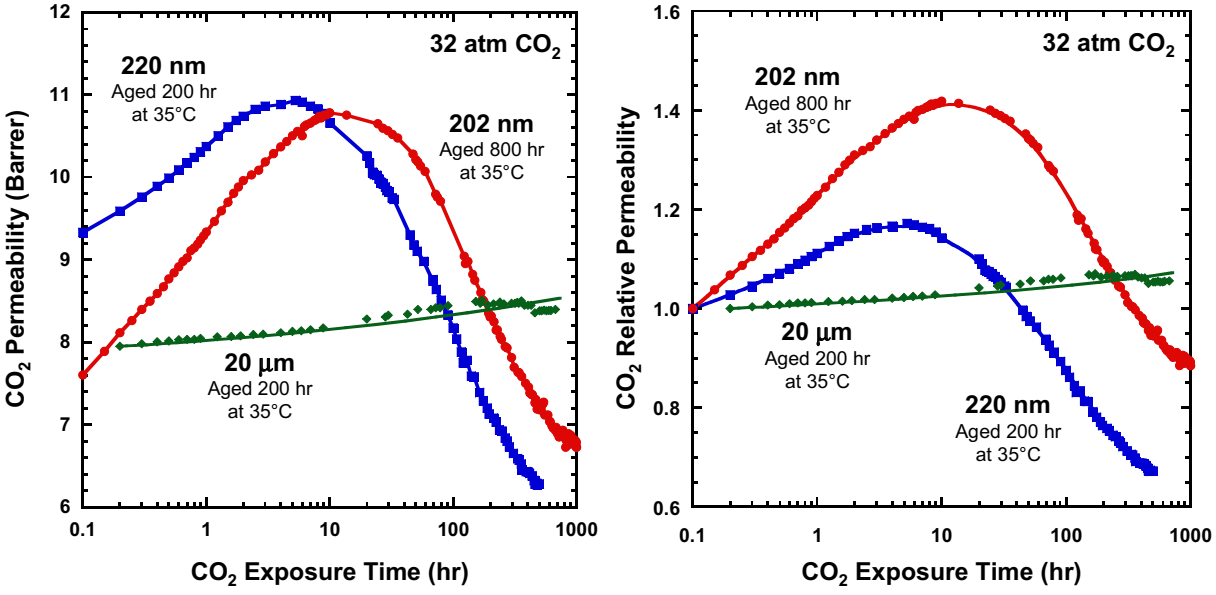

Fig. 8. Effect of aging time and thickness on long-time CO_2 exposure behavior.

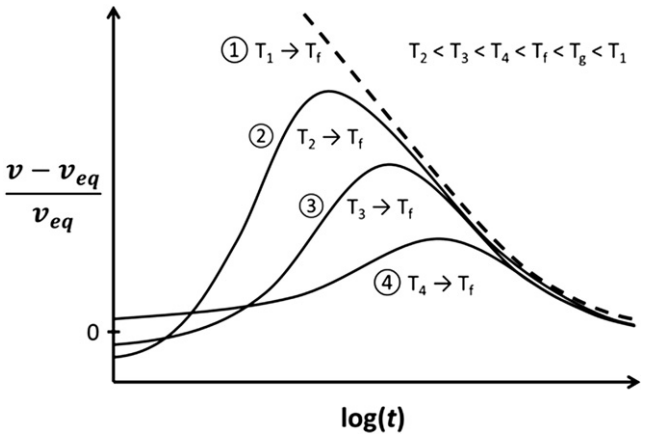

Fig. 9. Generalization of the Kovacs temperature jump experiment for glassy polymers. The response shows the deviation of sample volume (v) from its equilibrium volume (v_{eq}) at temperature T_f versus the time the sample has been at T_f following the various thermal histories explained in the text.

expected, whereas curves 2 to 4 show a maximum. For the latter, the polymer responds to the up-quench with an initial increase in volume, but then goes through a maximum as it begins to relax, eventually following the course of curve 1. Kovacs termed this a "memory" effect. McKenna and coworkers showed similar behavior induced by concentration jumps in either relative humidity or CO_2 [52–56]. In the glassy state, the polymer cannot respond immediately to the change in temperature, leading to the non-monotonic volumetric response in the case of opposing changes in temperature. The permeability vs. time plots in Fig. 7 represent a somewhat analogous situation as the concentration of plasticizing penetrant within the polymer changes, resulting in competition between two effects. First, the temperature quench to below T_g causes aging, manifesting itself by a tendency to decrease the permeability. Second, exposure to CO_2 tends to dilate the polymer, manifesting itself by a tendency to increase the permeability. Neither stimulus causes an immediate response, owing to the slow dynamics of the glassy state. However, it appears that the tendency for physical aging dominates at long times. There is no doubt the presence of CO_2 affects the subsequent physical aging kinetics.

5. Conclusions

Thickness plays a critical role in the CO_2 plasticization and conditioning processes of glassy polymer films. Thin films are more sensitive to changes in CO_2 pressure, and the response becomes more intense at greater pressures. Permeability changes occur even at short time scales for thin films, as opposed to thick films which take nearly the same amount of time merely to reach steady state. The difference in relaxation time distribution between thick and thin films plays a significant role in the time dependence of CO_2 response. At moderate time scales, thin glassy polymer films undergo more rapid plasticization by CO_2, in contrast with thick films. This behavior is analogous to more rapid physical aging of thin films. Moreover, the conventionally defined "plasticization pressure" is not adequate to determine when plasticization begins. Plasticization in thin films is strongly dependent on aging time of a film, whereas thick films show little change with aging time. Permeability data for O_2, N_2, and CH_4following CO_2 exposure indicates that thinner films experience greater changes in gas permeability in response to prior sorption of CO_2, i.e., "conditioning" effects, than do thick films, but the effect on selectivity is unclear. Thus, CO_2 transport data from thick films cannot fully predict thin film behavior. The CO_2 response of thin films is dependent on thickness, aging time, CO_2 pressure, exposure time, and prior history.

At longer CO_2 exposure times, thin films behave much differently than thick films. Initially, thin films exhibit a large increase in CO_2 permeability, but the trend eventually reverses and the films decrease in permeability to a significant extent. This is attributed to competition between the CO_2 plasticization effect and physical aging, and the behavior resembles the volume recovery "memory effect" observed by Kovacs. Thick films do not seem to reach a well-defined maximum within the experimental timescale. This behavior has yet to be fully explained, and other investigations are needed to determine its cause.

Acknowledgments

The authors gratefully acknowledge the U.S. Department of Energy for the generous funding of this project.

References

[1] Koros WJ, Paul DR. Polym Eng Sci 1980;20:14–9.
[2] Vieth WR, Howell JM, Hsieh JH. J Membr Sci 1976;1:177–220.
[3] Sanders ES. J Membr Sci 1988;37:63–80.
[4] Chiou JS, Paul DR. J Membr Sci 1987;32:195–205.
[5] Chiou JS, Barlow JW, Paul DR. J App Polym Sci 1985;30:2633–42.
[6] Wessling M, Schoeman S, van Der Boomgaard T, Smolders CA. Gas Sep Purif 1991;5:222–8.
[7] Chern RT, Provan CN. Macromolecules 1991;24:2203–7.
[8] Wonders A, Paul DR. J Membr Sci 1979;5:63–75.
[9] Struik LCE. Physical aging. In: Amorphous polymers and other materials. Amsterdam, The Netherlands: Elsevier Scientific Publishing Company; 1978.
[10] Pfromm PH, Koros WJ. Polymer 1995;36:2379–87.
[11] Dorkenoo KD, Pfromm PH. Macromolecules 2000;33:3747–51.
[12] McCaig MS, Paul DR. Polymer 2000;41:629–37.
[13] McCaig MS, Paul DR, Barlow JW. Polymer 2000;41:639–48.
[14] Huang Y, Paul DR. J Membr Sci 2004;244:167–78.
[15] Huang Y, Paul DR. Polymer 2004;45:8377–93.
[16] Huang Y, Paul DR. Macromolecules 2006;39:1554–9.
[17] Huang Y, Wang X, Paul DR. J Membr Sci 2006;277:219–29.
[18] Bos A, Pünt IGM, Wessling M, Strathmann H. J Membr Sci 1999;155:67–78.
[19] Ismail AF, Lorna W. Sep Purif Technol 2002;27:173–94.
[20] Wind JD, Sirard SM, Paul DR, Green PF, Johnston KP, Koros WJ. Macromolecules 2003;36:6433–41.
[21] Wind JD, Paul DR, Koros WJ. J Membr Sci 2004;228:227–36.
[22] Kanehashi S, Nakagawa T, Nagai K, Duthie X, Kentish S, Stevens G. J Membr Sci 2007;298:147–55.
[23] Berens AR. Polymer 1977;18:697–704.
[24] Berens AR. J Membr Sci 1978;3:247–64.
[25] Berens AR. Polym Eng Sci 1980;20:95–101.
[26] Berens AR. ACS Sym Ser Barrier Polym Structures 1990;423:92–110.
[27] Berens AR, Hopfenberg HB. Polymer 1978;19:489–96.
[28] Berens AR, Hopfenberg HB. J Polym Sci Part B Polym Phys 1979;17:1757–70.
[29] Wessling M, Lopez ML, Strathmann H. Sep Purif Technol 2001;24:223–33.
[30] Zhou C, Chung T-S, Wang R, Liu Y, Goh SH. J Membr Sci 2003;225:125–34.
[31] Pfromm PH, PhD Thesis, University Of Texas at Austin; 1994.
[32] Scholes CA, Chen GQ, Stevens GW, Kentish SE. J Membr Sci 2010;346:208–14.
[33] Chung T-S, Cao C, Wang R. J Polym Sci Part B Polym Phys 2004;42:354–64.
[34] Kim JH, Koros WJ, Paul DR. Polymer 2006;47:3094–103.
[35] Kim JH, Koros WJ, Paul DR. Polymer 2006;47:3104–11.
[36] Kim JH, Koros WJ, Paul DR. J Membr Sci 2006;282:21–31.
[37] Kim JH, Koros WJ, Paul DR. J Membr Sci 2006;282:32–43.
[38] Kratochvil AM, Damle-Mogri S, Koros WJ. Macromolecules 2009;42:5670–5.
[39] Kratochvil AM, Koros WJ. Macromolecules 2010;43:4679–87.
[40] Lee JS, Madden WC, Koros WJ. J Membr Sci 2010;350:232–41.
[41] Lee JS, Madden WC, Koros WJ. J Membr Sci 2010;350:242–51.
[42] Pandiyan S, Brown D, Neyertz S, a van der Vegt NF. Macromolecules 2010;43:2605–21.
[43] Neyertz S, Brown D, Pandiyan S, a van der Vegt NF. Macromolecules 2010;43:7813–27.
[44] Rowe BW, Freeman BD, Paul DR. Polymer 2010;51:3784–92.
[45] Henis JM, Tripodi MK. Science 1983;220:11–7.
[46] Rowe BW, Freeman BD, Paul DR. Polymer 2009;50:5565–75.
[47] Koros WJ, Paul DR, Rocha AA. J Polym Sci Part B Polym Phys 1976;14:687–702.
[48] Puleo AC, Muruganandam N, Paul DR. J Polym Sci Part B Polym Phys 1989;27:2385–406.
[49] Puleo AC, Paul DR, Kelley SS. J Membr Sci 1989;47:301–32.

[50] Jordan S, Koros WJ, Fleming G. J Membr Sci 1987;30:191–212.
[51] Kovacs AJ, Hutchinson JM, Aklonis JJ. The structure of non-crystalline materials. London: Taylor & Francis; 1977. 153–163.
[52] Alcoutlabi M, Banda L, McKenna GB. Polymer 2004;45:5629–34.
[53] Zheng Y, McKenna GB. Macromolecules 2003;36:2387–96.
[54] Zheng Y, Priestley RD, McKenna GB. J Polym Sci Part B Polym Phys 2004;42:2107–21.
[55] McKenna GB. J Non-Cryst Solids 2007;353:3820–8.
[56] Alcoutlabi M, Briatico-Vangosa F, McKenna GB. J Polym Sci Part B Polym Phys 2002;40:2050–64.